



CrossMark
click for updates

Cite this: *Lab Chip*, 2015, 15, 3314

Functionalization of micromodels with kaolinite for investigation of low salinity oil-recovery processes†

Wen Song and Anthony R. Kovscek*

Sandstone formations are ubiquitous in both aquifers and petroleum reservoirs, of which clay is a major constituent. The release of clay particles from pore surfaces as a result of reduced injection fluid salinity can greatly modify the recovery of hydrocarbons from subsurface formations by shifting the wettability properties of the rock. In this paper we demonstrate a microfluidic approach whereby kaolinite is deposited into a two-dimensional microfluidic network (micromodel) to enable direct pore-scale, real-time visualization of fluid–solid interactions with representative pore-geometry and realistic surface interactions between the reservoir fluids and the formation rock. Structural characterization of deposited kaolinite particles agrees well with natural modes of occurrence in Berea sandstones; hence, the clay deposition method developed in this work is validated. Specifically, more than 90% of the deposited clay particles formed pore-lining structures and the remainder formed pore bridging structures. Further, regions of highly concentrated clay deposition likely leading to so-called Dalmatian wetting properties were found throughout the micromodel. Two post-deposition treatments are described whereby clay is adhered to the silicon surface reversibly and irreversibly resulting in microfluidic systems that are amenable to studies on (i) the fundamental mechanisms governing the increased oil recovery during low salinity waterfloods and (ii) the effect of a mixed-wet surface on oil recovery, respectively. The reversibly functionalized platform is used to determine the conditions at which stably adhered clay particles detach. Specifically, injection brine salinity below 6000 ppm of NaCl induced kaolinite particle release from the silicon surface. Furthermore, when applied to an aged system with crude oil, the low salinity waterflood recovered an additional 14% of the original oil in place compared to waterflooding with the formation brine.

Received 14th May 2015,
Accepted 23rd June 2015

DOI: 10.1039/c5lc00544b

www.rsc.org/loc

Introduction

Rock wettability is a key determining factor in the recoverability of oil from the subsurface. A clean, unaltered sandstone is strongly water wet.¹ Clay, however, is oil wet.^{2,3} Naturally occurring sandstones that encompass petroleum reservoirs contain significant amounts of clay that are natively adhered to the surface of sand grains. Interaction between the clay particles, connate water, and specific components in the hydrocarbon drastically changes the transport of fluids in the subsurface.^{3–5} Oil-wet systems generally result in lower recovery factors compared to mixed-wet or water-wet systems for economic amounts of water injection.

Waterflooding is a recovery technique that is widely practiced to increase the recovery of hydrocarbons from the subsurface. Specifically, brines with various components (*e.g.*,

salts, acids, *etc.*) are commonly injected into hydrocarbon-containing formations to drive out the remaining oil. With the introduction of other fluids during secondary and tertiary recovery processes, primarily with the injection of brine that is compositionally dissimilar to the connate water, clay particles have been found to detach from the pore space and subsequently plug the available pore throats during their migration. In particular, the salinity and pH of the injected brine along with the temperature of the system have been found to play a significant role in the release of the fine clay particles from sand grains.^{5–7}

The literature presents several studies to delineate the fundamental mechanisms that cause clay particles to detach from the pore surface.^{5,6,8–10} Specifically, the DLVO (Derjaguin, Landau, Verwey, and Overbeek) theory has been applied to describe the interplay of attractive van der Waals forces and repulsive double layer forces between the clay particles and the sand grains; these interactions define the conditions at which clay particles are released. Effects such as the impact of cation species on clay detachment, however, are not well accounted for by the DLVO theory without other

Stanford University, Energy Resources Engineering, 367 Panama St, room 50, Stanford, California, USA. E-mail: kovscek@stanford.edu

† Electronic supplementary information (ESI) available. See DOI: 10.1039/c5lc00544b

considerations (*e.g.*, electroselectivity).¹¹ A mechanistic understanding of pore-level clay mobilization under different reservoir conditions is required.

Mobilized clay particles affect the reservoir, and ultimately the recovery of hydrocarbons, in a number of ways. Two important mechanisms by which detached clay significantly impacts subsurface flow are as follows. First, the flocculation of detached clay particles in the presence of low salinity brine results in larger particles that easily plug pore throats. Blocked pore throats drastically decrease the paths available for flow, and thus reduce the permeability of the formation and ultimately their recovery. This is known as formation damage.¹² Second, the release of oil-wet clay particles from the water-wet sand surface shifts the wettability of the system to one that is increasingly water-wet, and hence it increases the ability to recover hydrocarbons from the subsurface.¹³ Therefore, it is crucial to understand (i) the mechanisms that cause clay particles to detach from the pore space and (ii) the consequences resulting from their release and migration.

Understanding the pore-scale behavior is critical to the design and execution of effective oil-recovery schemes. Core-scale experiments have previously been conducted to study fluid-fines interactions and the effects of various parameters (*e.g.*, temperature, pH, and salinity of injection fluid) on clay detachment.^{2,3,6,9,11,14,15} Through these experiments, indirect measures of changes in the porous medium (*e.g.*, formation damage and wettability alteration) are deduced. Core experiments, however, are unable to capture the pore-scale events that dictate the low salinity effect. Advanced visualization techniques such as X-ray computed tomography (X-ray CT)¹⁶ and micro X-ray computed tomography (micro X-ray CT)¹⁷ are able to obtain pore-scale visualization in core flood experiments; however, whole-core scans can take up to 40 minutes, rendering them opaque to the dynamics of micro-scale clay detachment studies in the time frame that is required. Real-time pore-scale visualization of the interactions between fluids, grains, and clay particles is required to develop a fundamental understanding of the mechanisms that dictate recovery efficiency of hydrocarbons from the subsurface.

Microfluidics is an emerging technology that enables the direct visualization of pore-scale phenomena in real time.¹⁸ Recently, glass and silicon microfluidic devices with representative pore-scale geometries have enabled the study of fluid behavior in petroleum related applications.^{19–27} Specifically, microfluidic techniques have been applied in reservoir fluid property measurements such as the asphaltene content and solvent diffusion in crude oil.^{26,28–31} In particular, Buchgraber *et al.*, 2012, described the creation of two-dimensional microfluidic devices (micromodels) with a pore-scale geometry that is identical to real rocks using thin section images obtained with a scanning electron microscope (SEM). These micromodels allow for the direct visualization of flow behavior through a two-dimensional porous medium that is geometrically representative of a real rock. This approach however is limited by the lack of representative

surface heterogeneity that dictates pore-scale flow dynamics. Silicon and glass substrates, like the quartz grains that comprise the majority of sandstones, are strongly water wet. The presence of clays and their associated properties, however, are not represented in this micromodel. That is, previous micromodels could not replicate the presence of clays within the pore space and their influence on hydrocarbon recovery processes through phenomena such as (i) detachment in the absence of salt ions, (ii) fines migration, and (iii) their role in increasing recovery during low salinity waterflooding and in formation damage.

In this study, a process is developed to functionalize silicon micromodel by adding clay to pore surfaces. The resulting micromodel allows us to better understand the mechanisms dominating particle release and subsequent formation damage. In the following, a method for coating the micromodel with kaolinite – a non-swelling, dispersive clay typically present in sandstones – is described. Specifically, methods for depositing the clay both reversibly (*i.e.*, the clay is adhered to the silicon surface at high salinities but its attachment is sensitive to reductions in injection fluid salinity) and irreversibly (*i.e.*, the clay is attached to the pore surface and is insensitive to changes in the injection fluid salinity) are described. To validate the approach, the modes by which kaolinite particles were attached to the silicon surface were characterized and compared to their mode of occurrence in sandstones as indicated in the literature. Visualization experiments using the reversibly clay-coated micromodel show evidence of clay migration and of permeability reduction as a result of low salinity waterflooding. Furthermore, experiments involving crude-oil displacement resulted in wettability alteration of the system, emulsion generation, and increased oil recovery after low salinity waterflooding.

Experimental methods

Pore-scale visualization of the impact of salinity and temperature on clay mobility in sandstones was achieved using a two-dimensional microfluidic device with pore structures representative of those found in the reservoir rock. Specifically, the micromodel consists of a porous matrix that is 5 cm × 5 cm with an etch depth of 30 μm to allow for pore-scale flow visualization and inlet and outlet fractures to allow for even pressure fields. The porous matrix has an average coordination number of 4; that is, each pore is connected to 4 other pores, on average. These dimensions, given the pore geometry, provide ~300 × 300 pores, which far exceed the minimum number of pores required for representative elementary volume scaling in two dimensions.^{32,33} The microfluidic device (micromodel) used in this work was fabricated by etching the sandstone pore structure into a silicon wafer using standard photolithography techniques. Silicon and glass substrates were chosen due to their inherent water wettability and compositional similarity to sandstones. The etched silicon wafer was subsequently bonded to a piece of Schott Borofloat 33 glass (S.I. Howard Glass, Worcester, MA) through anodic

bonding; heating and exposure to oxygen generates a layer of silica (SiO_2), which is similar to quartz – the major component of sandstones – and creates a strongly water-wet pore space. The micromodel fabrication techniques here follow those in previously published work.¹⁹ The following section describes the novel method by which the surface of the pore space within the micromodel was functionalized using clay to obtain a system that is a good representative of a real reservoir and the subsequent treatments resulting in mobile and immobile clay particles.

Clay solution preparation and deposition into the micromodel

Deionized (DI) water was used to create a 15 000 ppm NaCl (Sodium Chloride, S271-3, Fisher Scientific) solution typical of formation brine. A 1 wt% clay suspension was prepared by adding kaolinite powder (Kaolin, K2-500, Fisher Scientific) to the vigorously stirred saline solution at atmospheric pressure. Kaolinite clay was chosen to replicate the initial conditions within the reservoir due to its prevalence in Berea sandstone and hydrocarbon reservoirs.⁶ Moreover, kaolinite is non-swelling in nature. That is, changes in the porous medium permeability are expected to be solely due to clay detachment from the silica surface, its migration, and its blockage of pores/pore throats.

The kaolinite powder was mixed with the high salinity reservoir brine in order to (i) deliver the kaolinite particles evenly into the microfluidic system without severe plugging (and consequently permeability reduction) and (ii) allow for sufficient clay adsorption on the silica surface because the presence of cations is critical to clay attachment, as explained by the DLVO theory.⁹ Specifically, it has been shown previously that the introduction of low salinity brine to a system initially in contact with high salinity brines can (i) increase oil recovery and (ii) stimulate fines migration.^{2,11,14,15} Furthermore, clay particles require the presence of specific cations in the aqueous phase in order to attach to the silica surface; the absence of the required ions lead to clay particle release, increased flocculation, and ultimately pore plugging (*i.e.*, formation damage).¹² The kaolinite mixture was stirred vigorously for 15 minutes until a homogeneous solution was obtained. The suspension was then sonicated (Bransonic 220) for one hour to disperse the kaolinite particles throughout the mixture and to prevent flocculation from occurring. A well-dispersed kaolinite solution delays premature particle settling in the fluid delivery tubing and enables injection into the micromodel without significant plugging at the inlet fracture.

The experimental setup is shown in Fig. 1. Deionized water was injected into the micromodel using a 12 mL syringe (Monoject) and a syringe pump (Harvard Apparatus, Holliston, MA) to displace the initial gas phase at a superficial velocity of 30 m per day. The syringe pump was nominally pulseless and a stainless steel syringe (no stick-slip of moving parts on the cylinder wall) was used to inject the

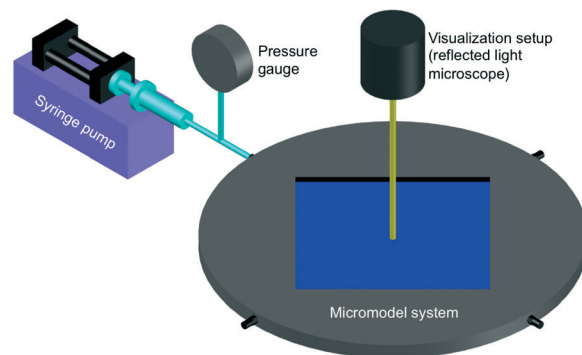


Fig. 1 Experimental setup for visualizing the mobility of clay particles within the micromodel. Saline solutions were injected using a syringe pump at a constant superficial velocity of 30 m per day. The syringe pump used was nominally pulseless and a stainless steel syringe was used to avoid stick-slip effects during injection. The microfluidic system was open to atmosphere downstream. Clay detachment was detected by monitoring the clay particles in the pore space at 25 fixed locations distributed evenly across the micromodel over time.

saline fluids to minimize pressure pulses during experiments. Fluids were delivered at a constant flow rate, with the outlets open to the atmosphere. All experiments were conducted at room temperature. The fluid behavior within the microfluidic system was visualized under brightfield imaging using a reflected light metallurgical microscope (S/N: MT1000T2006120001), and images were captured using a mounted camcorder (Canon VIXIA HF S200 HD Camcorder). The microfluidic system was continuously flushed with deionized water until all trapped gas bubbles were displaced by or dissolved into the aqueous phase. After the micromodel was fully saturated with water (no more gas phase present), several pore volumes of deionized water were flowed through to ensure that the system contained no other ions.

Once the micromodel was fully saturated with DI water as shown in Fig. 2(a), several pore volumes of the reservoir brine were injected using the syringe pump. The motivation for this is twofold: (1) to replicate the connate water in the reservoir and (ii) to avoid clay flocculation during deposition as a result of low salinity shock. The well-dispersed kaolinite suspension was then injected using the syringe pump at a rate of 20 m per day for several pore volumes to deposit a sufficient coating of kaolinite in the system. The optimal injection rate was found to be 20 m per day to minimize pressure buildup and maximize homogeneous clay deposition. To prevent plugging at the inlet fracture, the kaolinite suspension may be introduced while sonicating the micromodel. Sonicating the system during injection also aids in creating an evenly distributed clay coating within the micromodel; however, sonication for extended periods (*e.g.*, continuous sonication during kaolinite deposition) inhibits the clay from attaching to the surface of the micromodel.

Once the micromodel was sufficiently coated with clay, as shown in Fig. 2(b), the system was injected with air to remove plugged particles at the pore throats. The strong interfacial

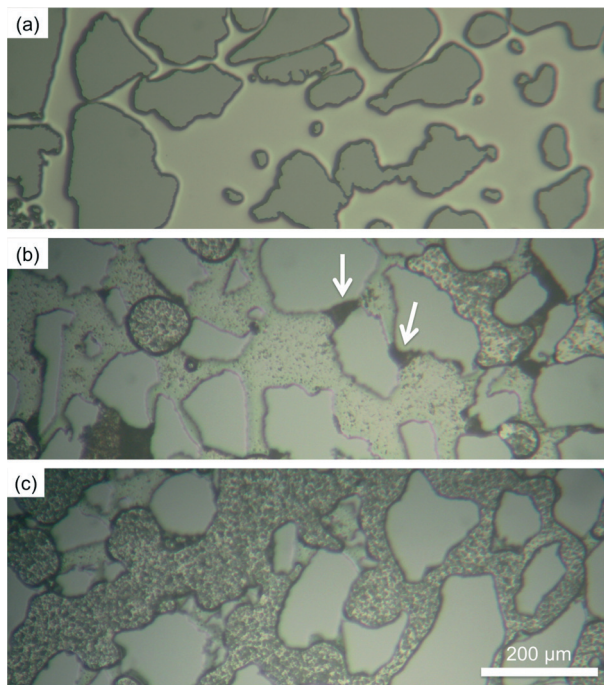


Fig. 2 Kaolinite deposition into micromodel pore space. (a) Water-saturated micromodel prior to clay introduction. (b) Some plugging is seen in pore throats after clay addition, which does not replicate well the initial conditions in the reservoir rock (refer to white arrows). (c) The throat-plugging clay particles are removed by the strong interfacial tension between the brine and the air, providing a clay coated silica surface that is a good representative of the reservoir rock.

tension between the air and the brine was able to dislodge throat-plugging clays as well as kaolinite particles that were not firmly attached to the silica surface. Fig. 2(c) shows the clay-coated micromodel that is a good representative of the reservoir rock, in which the pores are evenly coated with a significant amount of clay and with very few plugged pore throats.

Micromodel treatment determining clay mobility

After the dislodgement of throat-plugging kaolinite, the micromodel was treated in one of two manners to create a system in which (i) the clay may be mobilized in response to decreases in brine salinity or (ii) the clay is immobile in the system for all salinities. First, for the detachment studies conducted here, a reversible (mobile clay) system was desired. In this case, the microfluidic system was re-saturated and flushed with the initial reservoir brine at 20 m per day in order to eliminate any particles that were not adhered to the grain surface. Brine flooding was conducted for several pore volumes and images were taken at a fixed location until no more changes in the deposited clay could be observed.

Second, for wettability alteration studies requiring the presence of immobilized clay in the pore space, an irreversible system was desired. Consequently, the silicon surface

was functionalized through heating the vacuum-dried micromodel. The clay-coated micromodel was placed on a hot plate that was initially at room temperature and heated gradually to 120 °C for 25 minutes. This treatment ensured that the clay particles were firmly attached to the micromodel surface, while the temperature does not induce chemical degradation of the clay.³⁴ It was critical for the micromodel to be drained of water (saturated with air) in order to avoid breaking the micromodel due to the rapid volume expansion and subsequent pressure buildup from boiling during heating. The heated micromodel was then allowed to cool and was ready for visualization experiments to demonstrate the irreversibility of this process (*i.e.*, its lack of clay particle detachment in response to low salinity water).

Sensitivity experiments of salinity on clay detachment

Deionized water was used to create NaCl solutions at concentrations spanning the range of salinities typically used during secondary and tertiary recovery processes. Specifically, for each low salinity sensitivity experiment, the micromodel was flooded with the initial reservoir brine (15 000 ppm of NaCl) followed by the reduced salinity brine. Salt concentrations in the reduced salinity brines ranged from 8000 ppm to 0 ppm of NaCl (fresh water) in decrements of 2000 ppm. The low salinity solutions were injected into the micromodel to study the sensitivity of clay detachment from the pore surface in response to reduction in NaCl concentration. The solutions were delivered at constant flow rates corresponding to a superficial velocity of 30 m per day. Each saline solution was injected for 1 hour to allow for sufficient interaction between the solids and the fluids. For each waterflood that did not result in clay detachment, high salinity brine (15 000 ppm of NaCl) was injected to generate the initial conditions for the next experiment. In each experiment, the sensitivity of clay detachment to brine salinity was determined by visualizing the clay particles through the microscope in real time. Images were taken at the same location (for both high and low salinity brines) to isolate changes in the attached clay. The microfluidic system was maintained at atmospheric pressure downstream.

For reuse purposes, the micromodel was most effectively cleaned by alternating 1 M nitric acid (CAS: 7697-37-2, Sigma-Aldrich) injection with air injection for multiple pore volumes such that the strong interfacial tension between the gas and liquid phases could sweep away the particles loosened by acid. Sonication of the micromodel during acid injection aided the cleaning process by preventing the mobilized clay particles from flocculating or reattaching to the pore spaces downstream.

Waterflooding experiments on low salinity effect

For studies on the effect of injection fluid salinity on oil recovery, formation brine and crude oil were introduced to the reversibly kaolinite-coated micromodel to replicate the

Table 1 Composition of brine used to simulate the initial reservoir conditions

Reagent	Concentration (g L ⁻¹)
CaCl ₂ ·2H ₂ O (calcium chloride dihydrate)	0.183
MgCl ₂ ·6H ₂ O (magnesium chloride hexahydrate)	0.585
NaCl (sodium chloride)	20.461
KCl (potassium chloride)	0.611
Na ₂ SO ₄ (sodium sulfate)	0.109

initial reservoir conditions. Table 1 lists the composition of the brine chosen.

The vacuum dried micromodel (*i.e.*, micromodel that was reversibly coated with clay) was continuously flushed with several pore volumes of the brine using the syringe pump to create a fully water saturated system. The motivation for saturating the micromodel with brine typical of a reservoir was twofold: (1) to replicate the connate water in the reservoir and (ii) to avoid clay detachment as a result of low salinity shock.

Once the microfluidic system was fully saturated with the initial reservoir brine, crude oil was injected into the micromodel at 30 m per day and images were taken to observe the drainage process. The properties of the crude oil are as listed in Table 2. The interactions between kaolinite and the acid/base groups and asphaltenes in the crude oil are critical to the wettability alteration of the system, and thus crude oil was chosen in this study as opposed to mineral oils. Crude oil was injected for several pore volumes and water saturation was monitored over time until such a point at which the residual water saturation remained constant. The microfluidic system was then set aside and allowed to age for two weeks under ambient conditions to allow for sufficient interaction between the crude oil and the kaolinite particles to alter the silicon surface towards oil wettability. The resulting system was deemed the initial reservoir conditions.

After the microfluidic system was aged, a high salinity waterflood was performed followed by a freshwater waterflood to study the low salinity effect. The high salinity waterflood consisted of injecting the synthetic reservoir brine (as listed in Table 1) at a rate that corresponds to a superficial velocity of 30 m per day. The water and oil saturation was continuously monitored using the microscope setup. The high salinity waterflood was continued until the water saturation plateaued (*i.e.*, no incremental increases in water saturation was observed). The plateau corresponded to the residual

oil saturation as a result of the high salinity waterflood. Subsequently, the micromodel was injected with fresh water under the same conditions as the high salinity waterflood and images were taken at fixed locations before and after the freshwater flood to visually determine any additional oil recovery from the system.

Results and discussion

Micromodels coated with kaolinite reversibly (mobile clay particles for detachment sensitivity studies) and irreversibly (heat-facilitated immobilization of clay particles for wettability alteration studies) were created. Specifically, initiation of clay mobilization was (i) observed for brines with salinities between 6000 and 4000 ppm of NaCl in the reversibly coated system, in agreement with core-flooding experiments for Berea sandstones, and (ii) not observed for any salinities for the irreversibly coated micromodel. Further, the presence of clay was found to drastically change the pore-space wettability properties from strongly water-wet to mixed-wet and resulted in increased oil recovery after low salinity waterflooding.

With respect to the locations where fines were deposited, clay accumulation patterns were well-correlated with the *in situ* flow conditions. In general, very little clay deposition

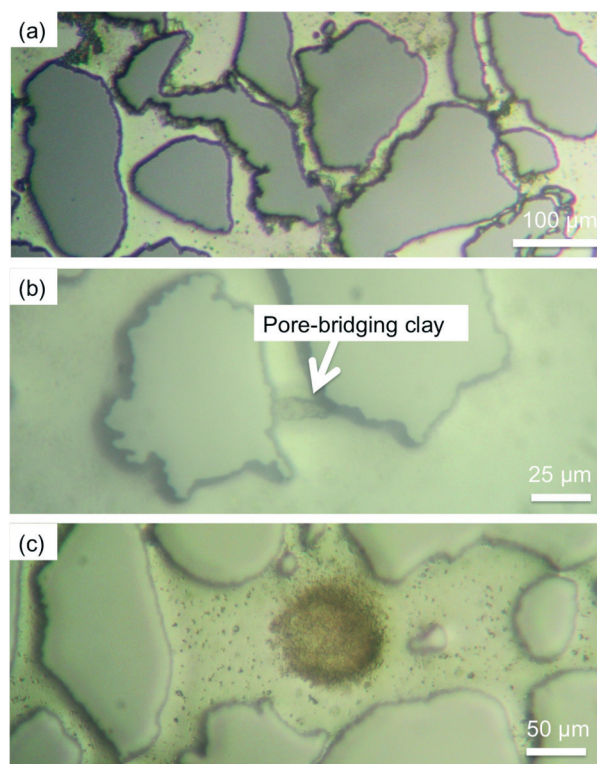


Fig. 3 Clay deposition structures and their incidence as a percent of total clay in the micromodel. Kaolinite was most commonly deposited (>90%) as discrete particles and in pore lining structures (a), while the remainder formed pore-bridging structures (b) as well as heterogeneous structures (c).

Table 2 Crude oil characterization³⁵

Crude oil properties	Value
Acid number (mg g ⁻¹)	2.36
Base number (mg g ⁻¹)	6.02
Asphaltene content (wt%)	2.69
Density (°API)	21
Viscosity at 22.8 °C (cP)	105.7

occurred in high velocity flow paths. Minimal deposition in the high velocity regions occurred as pore-bridging structures as a result of mechanical pore blockage under high flow velocities. Interestingly, Fig. 3(b) shows that large, plate-like kaolinite crystals overlapped one another to form bridge structures across narrow pore throats (high velocity paths). The high degree of connectivity between the pores (coordination number ~ 4) and a large number of pores in the system gives rise to flow both in series and in parallel. Pore-scale flow simulation of this system, however, shows that the predominant direction of transport is in series, in accordance with the imposed pressure drop across the micromodel (see Fig. S1 in the attached ESI† for a velocity map). Furthermore, the flow here is single-phase and is approximated as incompressible and at steady state. As such, fluid velocity is significantly larger through narrow pore throats, as required to carry the large particles before mechanical immobilization. Pore-bridging clay structures were not found across wide pore throats (low velocity regions). Significant clay deposition was found in enclosed low velocity regions immediately adjacent to high velocity paths where the clay particles are being carried into the pore space by the high-energy fluid and are then propelled into and retained in the enclosed stagnant regions due to the lack of flow. Minimal clay deposition, however, was observed in open stagnant regions due to the absence of a trapping mechanism to retain the free particles. Similar deposition patterns were observed for different positions with the same grain structure, further suggesting the dependence of clay deposition on carrier fluid velocity.

Sediment transport is commonly characterized by the Rouse number, $P = w_s/\kappa u^*$, where w_s is the particle fall velocity, $\kappa = 0.41$ is the von Karman constant, and u^* is the shear velocity of the flow. Specifically, the Rouse number is a dimensionless number that compares the rate at which particles fall *versus* the shear velocity of the flow that is keeping the particles in suspension. The experimental conditions during kaolinite deposition correspond to a Rouse number of ~ 0.2 , where particles are expected to be transported as wash load under which the flow velocity far exceeds the maximum velocity required for particles to settle. The significant deposition of pore-lining clays in the experiments, however, suggests that the ionic strength of the solution is the key driving force for particle attachment, as opposed to flow shear rates.

Clay structures were characterized and compared to those in naturally occurring sandstones to validate the deposition method developed. Specifically, discrete particles/pore-lining structures and pore-bridging clay structures were observed, as shown in Fig. 3(a) and (b), respectively. Furthermore, anomalous deposits of kaolinite were also observed in which clay was concentrated within specific regions, as shown in Fig. 3(c). These patches of discontinuous mineralogy may lead to the formation of Dalmatian wetting patterns, *cf.*, Cueic (1991).³⁶ It was found that discrete particles and pore lining structures (Fig. 3(a)) were the most prevalent modes for attachment to the silica surface, accounting for $\sim 90\%$ of the total kaolinite particles deposited into the micromodel,

while pore bridging structures rounded out the remainder of the deposited clay. These results are consistent with kaolinite occurrence in sandstone cores as reported in the literature,³⁷ and demonstrate that the deposition method described here resulted in a pore space that was structurally representative of a clay-rich sandstone.

To validate the wettability characteristics of the clay-coated micromodel, 15 000 ppm NaCl brine was introduced to the initially dry micromodel under spontaneous imbibition conditions. Specifically, the spontaneous imbibition experiments showed that while the brine was able to penetrate the vast majority of the pore space, the anomalous clay clusters were extremely non-wetting to brine (in the presence of air) upon re-introduction. Fig. 4(a) shows a vacuum-dried micromodel with anomalous clay clusters, and Fig. 4(b) shows the same location after 2 minutes of spontaneous imbibition with 15 000 ppm NaCl brine. It is evident that the brine did not easily penetrate the pores where the highly concentrated clay clusters were located. In fact, after some time of spontaneous imbibition, the water–air interface closely followed the outline of the clay clusters, clearly demonstrating that the system has shifted from being homogeneously water-wet to heterogeneously mixed-wet.

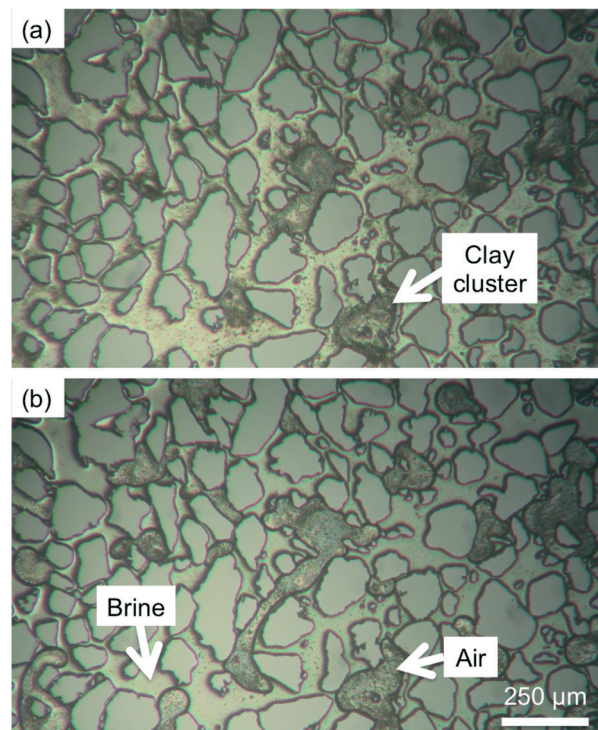


Fig. 4 Dry anomalously concentrated regions of kaolinite as shown in (a) is spontaneously imbibed with 15 000 ppm NaCl brine in (b). The initial phase is air, shown in (a), with significant deposits of kaolinite clusters. Upon spontaneous imbibition of brine, shown in (b), the kaolinite clusters are extremely non-wetting to water in the presence of air. Note the water–air interface in (b) that contours the kaolinite clusters. The water does not generally cross the circular outline of the kaolinite cluster during spontaneous imbibition.

Sensitivity of reversibly deposited clay to salinity

Initiation of significant fines release from the pore surface was visualized for injection brine salinities between 6000 and 4000 ppm of NaCl, in alignment with core experiments in Berea sandstones where the critical salt concentration for kaolinite release was found to be around 4000 ppm of NaCl.^{8,11} The effect of injection fluid salinity on kaolinite detachment from the silicon surface was quantified by injecting brine through the micromodel at a constant flow rate corresponding to a near-well superficial velocity of 30 m per day. The micromodel was imaged at 25 predetermined locations to visualize any changes in clay deposits. Low salinity brines with NaCl concentrations of 8000 ppm, 6000 ppm, 4000 ppm, 2000 ppm, and 0 ppm were injected into the clay-coated micromodel, in that order. The sensitivity of the attached kaolinite to salt ion concentration in the system was directly visualized using a microscope to identify the critical salt concentration at which kaolinite detaches from the silicon surface.

Images were taken at 25 fixed locations evenly distributed throughout the micromodel under initial reservoir conditions (15 000 ppm of NaCl) and during reduced salinity brine injection to identify the salinity at which clay particles are released. Quantitative analysis of the collective set of images is shown in Fig. 5(a) using image analysis. Effluent analysis was difficult to perform due to the microscale of the system. The strength of this method, however, is in enabling the direct visualization of clay detachment; this is not possible with conventional core flooding experiments that require effluent analysis. Fig. 5(a) shows the fraction of the pore space whereby clay particles were mobilized due to changes in NaCl concentration for various locations throughout the visualization platform. No clay mobilization was observed for injection brine concentrations above 6000 ppm of NaCl. At 6000 ppm of NaCl, however, minor clay particle detachment and migration were observed after the low salinity brine was injected. Specifically, the observed clay mobilization was confined within ~15 pore spaces of the inlet. Fig. 5(a) shows a sharp rise in the fraction of mobilized clay particles after flooding with 4000 ppm NaCl brine, corresponding to the significant clay detachment observed. These observations are consistent with those of core flooding in Berea sandstones and hence validate the method developed here.^{7,11} Pore-scale heterogeneities invariably introduce discrepancies from one pore to another; the collective analysis obtained using images at the 25 fixed locations throughout the micromodel, however, provides a good generalization for the system observed. The error associated with image analysis was small; the largest uncertainty associated with the data as displayed by the error bar corresponds to 0.9 ± 0.05 at 4000 ppm of NaCl. That is, all other error bars were less than this. Fig. 5(b) and (c) show the micromodel before and after 1 hour of 4000 ppm NaCl brine injection. Specifically, Fig. 5(c) shows that clay particles (i) were stripped from large channels and (ii) were re-deposited in regions with large pore body to pore throat

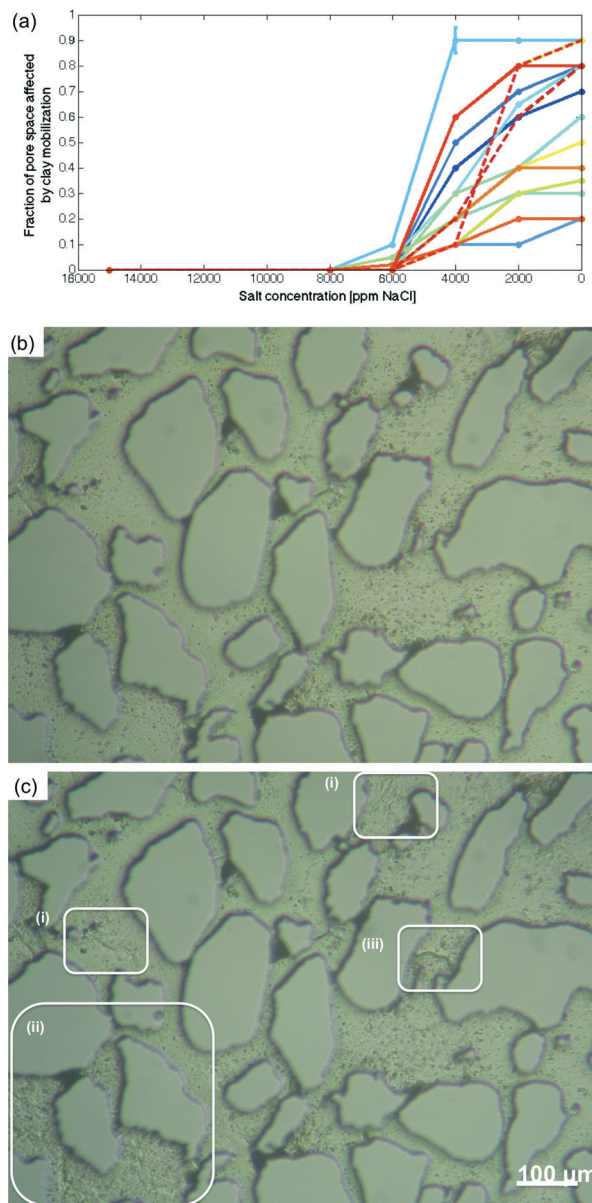


Fig. 5 Clay detachment from the silicon pore surface in response to changes in salt concentration. Image (a) shows the fraction of mobilized clay particles within the pore space at different salt concentrations for various locations throughout the micromodel determined through image analysis. The reverse lower axis shows the progression of low salinity waterflooding (high to low salinity). The largest error associated with the data as displayed by the error bar corresponds to 0.9 ± 0.05 at 4000 ppm of NaCl. Mobilization of clay particles was observed for salinities below 6000 ppm of NaCl. High fractions of mobilized clay were found in regions corresponding to preferential flow paths where the low salinity brine was delivered effectively through advection, whereas low clay mobilization was found in regions corresponding to stagnant flow conditions where salt dilution was mostly driven by diffusion. Mobilization of clay particles is determined by direct visualization of the pore space (b) before and (c) after a low salinity waterflood with 4000 ppm of NaCl. Significant kaolinite particle migration was observed. Pore-lining particles were drastically reduced in large channels (i), while deposition in regions with high pore body to pore throat size ratios was observed (ii). Furthermore, a large number of pore-bridging particles were found after the low salinity waterflood (iii).

ratios. These patterns resemble those of sedimentation in macro-systems such as riverbeds. Moreover, a significant increase in the number of large pore-bridging structures (spanning one to 3 pores) was found after the system was in contact with 4000 ppm NaCl brine, as highlighted in Fig. 5(c, iii). These large bridge configurations were the most predominant structures after the pore space was in contact with brine below 4000 ppm of NaCl. The formation of the large bridging structures corresponds well to a decrease in injectivity of brine into the micromodel, suggesting a negative impact on the transport of fluids with decreased salinity brine injections. Drastic clay mobilization was observed throughout the entirety of the micromodel after both 2000 ppm NaCl brine and freshwater (0 ppm of NaCl) flooding.

Fig. 5(a) shows that while the release of kaolinite from the silicon pore surface was induced after flooding with 4000 ppm NaCl brine throughout the direct visualization platform, the fraction of the affected pore space varied. The reverse lower axis serves to demonstrate that clay mobilization occurs only when a critical salt concentration has been reached. That is, the reverse lower axis shows the progression of waterflooding that goes from high salinity to low salinity. Specifically, high fractions of mobilized clay were found in regions corresponding to preferential flow paths, as determined through single-phase pore-scale flow simulations (see Fig. S1 in the ESI† for a velocity map), where the low salinity brine was delivered effectively through advection, whereas low clay mobilization was found in regions corresponding to stagnant flow conditions where salt dilution was mostly driven by diffusion. Pore-level permeability reductions due to the formation of bridging structures across preferential flow paths resulted in drastic increases in clay mobilization at lower salt concentrations, as shown by the cases denoted by the dashed lines in Fig. 5(a). These results confirm that the release of kaolinite particles from silicon is indeed sensitive to both the salt ion concentration in the system as well as the interstitial flow velocity. This, however, is in contrast to the experiments conducted by Khilar and Fogler, where the detachment of clay particles from a Berea sandstone core was found to occur around 4000 ppm of NaCl but was insensitive to flow rate for velocities between 4 m per day to 720 m per day.

Irreversibly deposited clay

The heat-treated microfluidic system was saturated with 15 000 ppm NaCl brine to replicate the initial reservoir conditions. The system – especially the clay particles – was found to be water-wetting. Specifically, cornering/crevice flow was observed during spontaneous imbibition where thin water films wet the clay patches before the bulk pore body was filled with water. This is in stark contrast with the unheated system, where the clay patches were extremely non-wetting to water (water could not infiltrate clay-dense pore bodies). Following brine saturation, fresh water (0 ppm of NaCl) was injected into the irreversibly coated micromodel. Images were

recorded at fixed locations throughout the micromodel before and after the freshwater flood. Clay mobilization was not observed after the freshwater flood; this demonstrates the permanent attachment of the clay particles to the silicon surface with respect to salt concentration after the heat treatment and validates the irreversible clay deposition method developed.

Injection fluid salinity and crude-oil recovery

The reversibly clay-coated micromodel was fully saturated with formation brine and injected with crude oil to replicate the initial reservoir conditions, as shown in Fig. 6. Image analysis shows that the connate water saturation was ~5%. The system was aged for two weeks to allow for sufficient interaction between the clay and the oil components. Immediately upon introducing the crude oil to the micromodel, as shown in Fig. 6(a), the oil–water interface was smooth and the system appeared to be strongly water-wet. After aging, however, “kinks” were observed in the water–oil interface where clay particles were located and localized oil-wet regions were observed, as shown in Fig. 6(b). This change is indicative of the altered wettability properties of the porous medium due to the affinity of kaolinite towards oil.

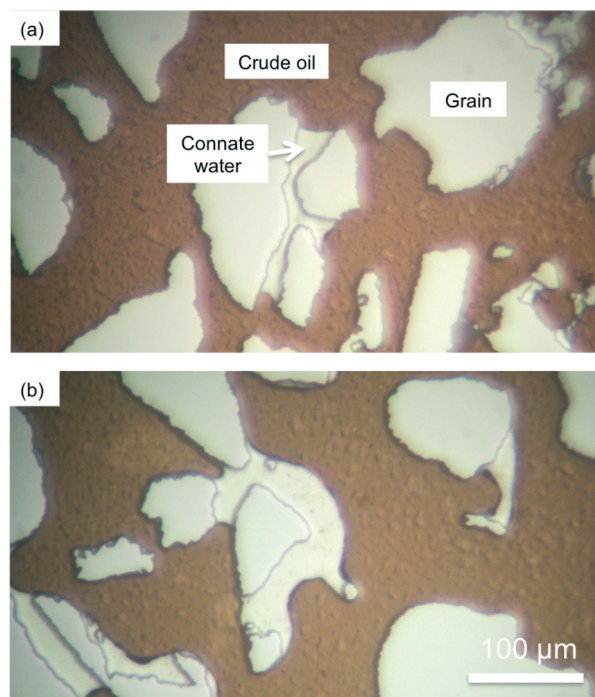


Fig. 6 Reversibly clay-coated micromodel representing initial reservoir conditions (a) immediately upon injection of oil and (b) after aging for two weeks. The system was filled with initial reservoir brine, followed by injection of crude oil. Crude oil was injected for several pore volumes and the water saturation of the system was monitored until such a point at which further injection of oil could not displace the residual water. The connate water saturation was ~5%. The water–oil interfaces are smooth curves pre-aging and are deformed by kinks about clay particles after aging, indicating a shift in the wettability properties of the system.

To study the effect of injection fluid salt concentration on oil recovery, high salinity (*i.e.*, the initial formation brine) and low salinity (deionized water) fluids were injected sequentially into the aged micromodel at a flow rate of 20 m per day until no further reductions in the oil saturation were observed. That is, the imaged oil phase remained immobile in the pore space with brine injection. The resulting systems were imaged at several locations to obtain representative residual oil saturation, as shown in Fig. 7(a) and (b). The segmented images shown in Fig. 7(c) and (d) were created using Image J to differentiate between the oil, aqueous, and solid phases. Specifically, thresholds were applied to each image and the interfaces between the oil, water, and solid phases were identified using the “find edges” function. The images were then binarized and analyzed to find the oil/water saturation. Non-uniform lighting and the presence of clay particles makes the process difficult to automate and thus individual treatment was applied. This approach was applied to quantify the oil and water saturation (volume fraction of oil or water in the pore space, $S_{oil} = A_{oil}/(A_{total} - A_{grains})$ and $S_{brine} = A_{brine}/(A_{total} - A_{grains})$, where the saturation sums to unity, $S_{oil} + S_{brine} = 1$). Residual oil saturation in the system as a result of the high and low salinity waterfloods was quantified in this manner. The residual oil saturation values after the high salinity brine flood and the low salinity freshwater flood were $S_{or} = 36\%$ and 22% , respectively. This recovery increase of 14% of the original oil in place provides direct evidence of improved oil recovery using freshwater flooding.

To understand the underlying mechanisms driving the increase in oil recovery, images were taken prior to (Fig. 8(a)) and during (Fig. 8(b)) the low salinity waterflood at fixed locations. It was found that the low salinity shock resulted in the

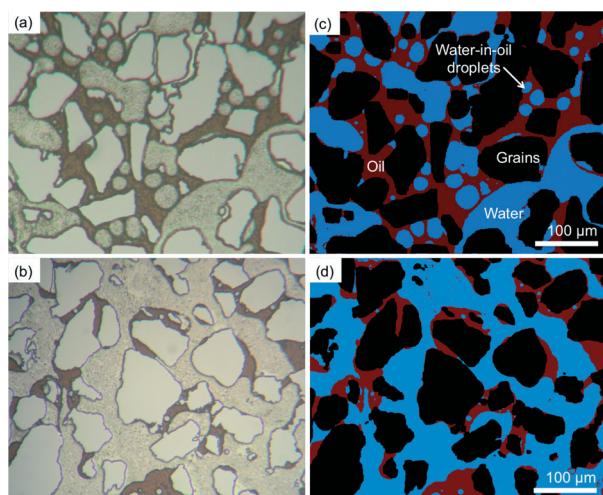


Fig. 7 Clay-coated micromodel after (a) high salinity (synthetic formation brine) flood and (b) low salinity (deionized water) flood. The water (blue), oil (red), and grains (black) are differentiated using image processing techniques in (c) and (d). The residual oil saturation values following the high salinity and low salinity waterfloods were $S_{or} = 36\%$ and 22% , respectively, indicating a 14% increase in oil recovery using deionized water.

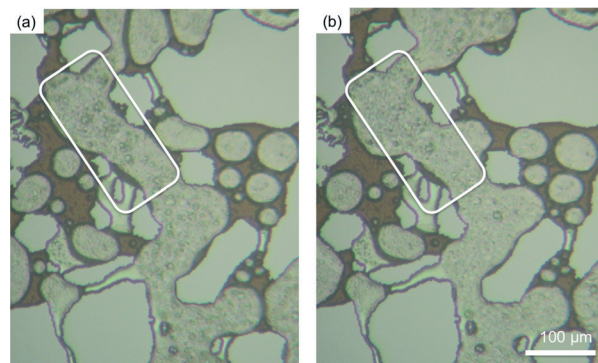


Fig. 8 Clay-coated micromodel before (a) and 5 minutes after (b) the low salinity waterflood. Clay particles appear to have relocated in the latter case, compared to the initial system.

rapid remobilization of adhered clay particles in the pore space that led to a subsequent increase in the water wettability of the porous medium. Fig. 9 shows images obtained using a confocal microscope (Sensofar S neox 3D optical profiler) that illustrate the four phenomena that contributed to the improved oil recovery of oil using low salinity flooding from the reversibly clay-coated micromodel. First, significant clay stripping at the pore-scale after the freshwater flood is shown, as indicated by the regions that are cleansed of clay in Fig. 9(a). This is consistent with low salinity flooding of sandstone cores.^{7,11} Second, the irregularly shaped oil–water interfaces in Fig. 9(b) demonstrate the wettability alteration of the micromodel to one that is mixed-wet. The altered wettability of the system is due to the introduction of the oil-wet clay particles in the pore space and the adherence of crude-oil components to that clay as well as adherence to other

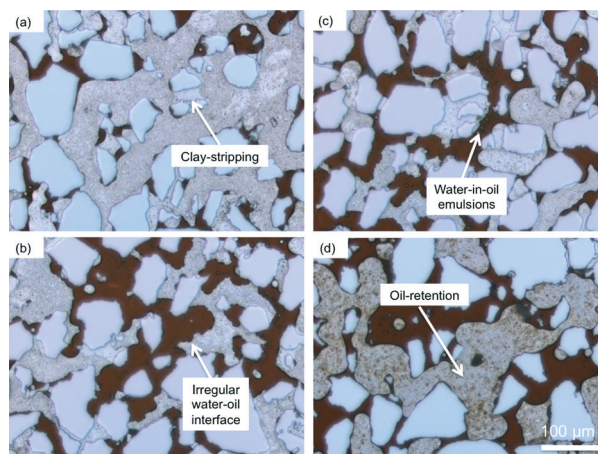


Fig. 9 Clay-coated micromodel following the low salinity waterflood imaged using a confocal microscope. Water-in-oil emulsions are found throughout the micromodel as shown in (a) and fit the macroscopic descriptions by Emadi *et al.*¹³ The oil–water interface in (b) is deformed due to the oil wettability of the kaolinite particles. Regions of clay stripping are observed in (c), similar to core-flooding experiments reported in the literature.⁷ Oil retention on clay particles is observed in (d) and fits the macroscopic inferences.³⁸ High resolution images are shown in the accompanying ESI.†

pore surfaces. Third, a large number of water-in-oil emulsions were found throughout the micromodel after the fresh-water flood, as shown in Fig. 9(c). Although there is disagreement within the literature on emulsion generation during low salinity flooding,¹³ the results here suggest that emulsions may be generated spontaneously during low salinity waterflooding. Fourth, immobile clays exhibited some oil retention, as observed in Fig. 9(d) indicated by the brown discoloration of the clay particles in the water phase. This, again, is due to the affinity of clay towards oil as opposed to water.³⁸ Overall, the four microscopic pore-scale observations described here appear to fit the inferences from macroscopic core-scale studies in sandstones.

Surface functionalized microfluidics enables direct visualization of the impact of fluid composition on the stability of kaolinite that is attached to sandstone surfaces. In particular, micromodels provide a direct means of visualizing the behavior of clay under a range of saline conditions. Specifically, pore-lining clay was found to have been removed from the surface of the grain, whereby exposing the water-wet surface and potentially aiding the recovery of hydrocarbons from such a system. Pore-bridging clay, however, was found to have been dislodged from the grain surface and had subsequently plugged pore throats downstream. Furthermore, mobile clay particles were found to have accumulated in small pore throats, especially those with pore-bridging clay structures impeding flow.

The work presented here provides the necessary groundwork for further studies in understanding the real-time fluid flow and fluid–solid interaction at the pore scale in real rocks. Specifically, this work is particularly amenable to the study of increased oil recovery as a result of the low salinity effect. Several directions are outlined for future work as follows.

First, it is desirable to map the mobilization characteristics of the clay functionalized silicon micromodel. Specifically, brine composition and fluid velocity sensitivity experiments should be conducted to determine the mobility of attached clay particles. Furthermore, three dimensional characterization of clay structures in the pore space using confocal microscopy can lead to a better understanding of the role that the various clay structures (pore lining, pore bridging, and anomalous structures) have in oil recovery. Specifically, the impact of clay mobilization during low salinity flooding is proposed to depend on the type of clay structure that is released. For example, the role that detached pore lining clays have in wettability change and consequently oil recovery is expected to differ from the role that pore bridging clays have in the low salinity flood. In the former, stripping the oil-wet clays from pore surface enhances the water wettability of the matrix and hence contributes to increased oil recovery, whereas in the latter, large pore bridging structures may flocculate to congest the available flow paths, hence resulting in formation damage. Furthermore, the formation of oil–water emulsions during low salinity flooding and its subsequent effects on the overall recovery mechanism is of interest. In

terms of oil recovery, changes in the micromodel wettability behavior due to clay can be studied by investigating the interactions between the oil, water, and clay particles during spontaneous and forced imbibition. Specifically, the salinity of the injection brine can be decreased to determine the effect of salinity on the imbibition process. Moreover, this study focused on the role that kaolinite – a predominant clay mineral present in sandstones that is non-swelling – has in fluid interactions in the pore space. Another important process, however, is the swelling and shrinking of clay particles. The work presented here provides the basis for future studies on the swelling and/or shrinking of clays, for example smectite and montmorillonite, under low salinity conditions.

Conclusion

In this study, we presented a method for depositing clay particles into micromodels as a means of creating a visualization platform with more representative surface interactions between the reservoir fluids and the formation rock. Specifically, the silicon micromodel was coated with kaolinite in two manners, reversibly and irreversibly, to enable the study of (i) the fundamental mechanisms governing the increased oil recovery during low salinity waterflooding and (ii) the effect of a mixed-wet surface on oil recovery, respectively. We demonstrated the successful deposition of kaolinite particles in the sandstone pore space, where the majority of clay deposited was pore lining (~90%) with the remainder forming pore-bridging structures across narrow pore throats. Furthermore, anomalous regions of highly concentrated clay deposits in the pore space were also observed and were found to be extremely non-wetting to water in the presence of air. High and low salinity brine injection in the micromodel identified the dependence of clay attachment and release on salt concentration. Formation brine and crude oil were introduced to the clay-coated micromodel and aged for two weeks to create the initial reservoir conditions and resulted in a mixed-wet pore space. High and low salinity brine floods were performed sequentially and image processing was applied to quantify the impact of injection fluid salinity on oil recovery. Specifically, the low salinity (deionized water) flood yielded a 14% increase in oil recovery after the high salinity flood.

Acknowledgements

The authors gratefully acknowledge funding from Chevron. Additional funding was provided by the Stanford University Petroleum Research Institute (SUPRI-A) affiliates. The authors thank Dr. Cyprien Soullaine for discussions that improved this work and for simulating the flow velocity maps. In addition, the authors gratefully acknowledge Dr. Cindy M. Ross for the discussions and help with the structures of clay in natural rocks and for designing the micromodel, Dr. Sophie Roman for help with micromodel fabrication, and Mr. Markus Zechner for helpful discussions.

References

- 1 A. R. Kovscek, H. Wong and C. J. Radke, A pore-level scenario for the development of mixed wettability in oil reservoirs, *AIChE J.*, 1993, **39**, 1072–1085.
- 2 A. Fogden, M. Kumar, N. R. Morrow and J. S. Buckley, Mobilization of fine particles during flooding of sandstones and possible relations to enhanced oil recovery, *Energy Fuels*, 2011, **25**, 1605–1616.
- 3 E. V. Lebedeva and A. Fogden, Adhesion of oil to kaolinite in water, *Environ. Sci. Technol.*, 2010, **44**, 9470–9475.
- 4 M. Yang, M. D. Annable and J. W. Jawitz, Back Diffusion from Thin Low Permeability Zones, *Environ. Sci. Technol.*, 2015, **49**, 415–422.
- 5 T. Tosco, A. Tiraferri and R. Sethi, Ionic Strength Dependent Transport of Microparticles in Saturated Porous Media: Modeling Mobilization and Immobilization Phenomena under Transient Chemical Conditions, *Environ. Sci. Technol.*, 2009, **43**, 4425–4431.
- 6 J. M. Schembre and A. R. Kovscek, Mechanism of Formation Damage at Elevated Temperature, *J. Energy Resour. Technol.*, 2005, **127**, 171.
- 7 G.-Q. Tang and N. R. Morrow, Influence of brine composition and fines migration on crude oil/brine/rock interactions and oil recovery, *J. Pet. Sci. Eng.*, 1999, **24**, 99–111.
- 8 K. S. Sorbie and I. R. Collins, A Proposed Pore-Scale Mechanism for How Low Salinity Waterflooding Works, in *SPE Improved Oil Recovery Symposium*, 2010, pp. 1–18, (Society of Petroleum Engineers).
- 9 J. M. Schembre, G.-Q. Tang and A. R. Kovscek, Wettability alteration and oil recovery by water imbibition at elevated temperatures, *J. Pet. Sci. Eng.*, 2006, **52**, 131–148.
- 10 F. Mugele, Ion adsorption-induced wetting transition in oil-water–mineral systems, *Sci. Rep.*, 2015, **5**, 10519.
- 11 K. C. Khilar and H. S. Fogler, The Existence of a Critical Salt Concentration for Particle Release, *J. Colloid Interface Sci.*, 1984, **101**, 214–224.
- 12 S. Berg, A. W. Cense, E. Jansen and K. Bakker, Direct Experimental Evidence of Wettability Modification By Low Salinity, in *International Symposium of the Society of Core Analysts*, 2009, pp. 1–12.
- 13 A. Emadi and M. Sohrabi, Visual Investigation of Oil Recovery by Low Salinity Water Injection: Formation of Water Micro-Dispersions and Wettability Alteration, in *SPE Annual Technical Conference and Exhibition*, 2013, pp. 1–15.
- 14 J. M. Schembre and A. R. Kovscek, Thermally Induced Fines Mobilization: Its Relationship to Wettability and Formation Damage, in *SPE International Thermal Operations and Heavy Oil Symposium*, 2004, pp. 1–16, (Society of Petroleum Engineers).
- 15 H. Mahani, S. Berg, D. Ilic, W. Bartels and V. Joekar-Niasar, Kinetics of Low-Salinity-Flooding Effect, *SPE J.*, 2015, **20**(1), 8–20.
- 16 B. Vega, A. Dutta and A. R. Kovscek, CT Imaging of Low-Permeability, Dual-Porosity Systems Using High X-ray Contrast Gas, *Transp. Porous Media*, 2014, **101**, 81–97.
- 17 P. Nguyen, H. Fadaei and D. Sinton, Microfluidics Underground: A Micro-Core Method for Pore Scale Analysis of Supercritical CO₂ Reactive Transport in Saline Aquifers, *J. Fluids Eng.*, 2013, **135**, 021203.
- 18 D. Sinton, Energy: the microfluidic frontier, *Lab Chip*, 2014, **14**, 3127–3134.
- 19 M. Buchgraber, A. R. Kovscek and L. M. Castanier, A Study of Microscale Gas Trapping Using Etched Silicon Micromodels, *Transp. Porous Media*, 2012, **95**, 647–668.
- 20 M. Buchgraber, M. Al-Dossary, C. M. Ross and A. R. Kovscek, Creation of a dual-porosity micromodel for pore-level visualization of multiphase flow, *J. Pet. Sci. Eng.*, 2012, **86–87**, 27–38.
- 21 W. Song, H. Fadaei and D. Sinton, Determination of Dew Point Conditions for CO₂ with Impurities Using Microfluidics, *Environ. Sci. Technol.*, 2014, **48**, 3567–3574.
- 22 W. Song, T. W. de Haas, H. Fadaei and D. Sinton, Chip-off-the-old-rock: the study of reservoir-relevant geological processes with real-rock micromodels, *Lab Chip*, 2014, **14**, 4382–4390.
- 23 M. Kim, A. Sell and D. Sinton, Aquifer-on-a-Chip: understanding pore-scale salt precipitation dynamics during CO₂ sequestration, *Lab Chip*, 2013, **13**, 2421–2662.
- 24 T. W. De Haas, H. Fadaei, U. Guerrero and D. Sinton, Steam-on-a-chip for oil recovery: the role of alkaline additives in steam assisted gravity drainage, *Lab Chip*, 2013, **13**, 3832–3839.
- 25 S. A. Bowden, P. B. Monaghan, R. Wilson, J. Parnell and J. M. Cooper, The liquid–liquid diffusive extraction of hydrocarbons from a North Sea oil using a microfluidic format, *Lab Chip*, 2006, **6**, 740–743.
- 26 S. A. Bowden, R. Wilson, J. Parnell and J. M. Cooper, Determination of the asphaltene and carboxylic acid content of a heavy oil using a microfluidic device, *Lab Chip*, 2009, **9**, 828–832.
- 27 S. A. Bowden, J. M. Cooper, F. Greub, D. Tambo and A. Hurst, Benchmarking methods of enhanced heavy oil recovery using a microscaled bead-pack, *Lab Chip*, 2010, **10**, 819–823.
- 28 M. H. Schneider, V. J. Sieben, A. M. Kharrat and F. Mostowfi, Measurement of asphaltenes using optical spectroscopy on a microfluidic platform, *Anal. Chem.*, 2013, **85**, 5153–5160.
- 29 F. Mostowfi, S. Molla and P. Tabeling, Determining phase diagrams of gas–liquid systems using a microfluidic PVT, *Lab Chip*, 2012, **12**, 4381–4387.
- 30 H. Fadaei, J. M. Shaw and D. Sinton, Bitumen–Toluene Mutual Diffusion Coefficients Using Microfluidics, *Energy Fuels*, 2013, **27**, 2042–2048.
- 31 A. Sell, H. Fadaei, M. Kim and D. Sinton, Microfluidic Approach for Reservoir-Specific Analysis, *Environ. Sci. Technol.*, 2013, **47**, 71–78.
- 32 A. R. Kovscek, G.-Q. Tang and C. J. Radke, Verification of Roof snap off as a foam-generation mechanism in porous media at steady state, *Colloids Surf., A*, 2007, **302**, 251–260.

- 33 F. A. L. Dullien, *Porous Media: Fluid Transport and Pore Structure*, Academic Press, 1992.
- 34 I. Bondino, S. Doorwar, R. Ellouz and G. Hamon, Visual microscopic investigations about the role of pH, salinity, and clay on oil adhesion, in *International Symposium of the Society of Core Analysts*, 2013, pp. 1–12.
- 35 J. Peng, *Heavy-Oil Solution Gas Drive and Fracture Reconsolidation of Diatomite During Thermal Operations*, Stanford University, 2009.
- 36 L. E. Cueic, in *Interfacial Phenomena in Oil Recovery*, ed. N. R. Morrow, Marcel Dekker New York, 1991, pp. 319–375.
- 37 J. W. Neasham, The Morphology of Dispersed Clay in Sandstone Reservoirs and Its Effect on Sandstone Shaliness Pore Space and Fluid Flow Properties, in *SPE Annual Fall Technical Conference and Exhibition*, 1977.
- 38 A. Lager, K. J. Webb, C. J. J. Black, M. Singleton and K. S. Sorbie, Low Salinity Oil Recovery – An Experimental Investigation, *Petrophysics*, 2008, **49**, 28–35.